Analysis of Auditory Attention Based EEG Signals across Time, Frequency and Time-Frequency Domains

Vanisha R. and Sushma S. Jagtap
Department of ECE, Rajalakshmi Engineering College, Chennai, Tamil Nadu, India

Keywords: Auditory Attention, Ensemble Classifiers, EEG, PhyAAt, Time-Frequency Domain.

Abstract: In this digital age auditory attention plays an important role in everything from flying an airplane to learning in a classroom environment. It is essential to focus on the user's or individual's auditory attention analysis because attention may differ while communicating with a non-native speaker and, in some cases, native speakers. Although there are many different types of physiological signals to analyze attention, EEG is the most widely used because this EEG signal is relatively simple and non-invasive. Among the numerous types of physiological datasets, the lack of study fails to auditory Attention to natural speech. This was complemented by the Physiology of Auditory attention to Speech Dataset, it was obtained from 25 healthy subjects by performing three separate tasks (resting, writing, and listening) at varied noise levels with native and non-native speakers. This study examines auditory attention in the time, frequency, and time-frequency domains while considering the all-noise level EEG data from three separate activities while interacting with native and non-native speakers. For this purpose, we employ a unique data segmentation preprocessing method that combines all EEG signals with specific window size and machine learning algorithms for task classification. The results show that the time-frequency domain surpasses the other domains.

1 INTRODUCTION

Auditory attention is a cognitive process that allows us to focus on certain sounds while ignoring others. This process can also influence other physiological responses, including heart rate and sympathetic tone (Scharf, B 2016). The Electroencephalogram (EEG) can be used to investigate brain activity, while the Photoplethysmogram (PPG) and Galvanic Skin Response (GSR) signals can be used to extract heart rate and sympathetic response (Val-Calvo, M., et al., 2020). EEG signals were used in our study to detect auditory attention because they are non-invasive and complex signals with numerous applications in biomedical fields such as sleep and brain-computer interface. Among the numerous types of physiological datasets, the absence of study fails to auditory Pay attention to natural speech.

The Physiology of Auditory Attention supplemented the Speech Dataset (Bajaj et al., 2020). The dataset includes three physiological signals recorded at a sampling rate of 128Hz from 25 healthy subjects performing three distinct tasks (resting, writing, and listening) under different noise levels, with both native and non-native speakers. The EEG signal is recorded with a 14-channel Emotive Epoc device. Two signals of Galvanic Skin Response (GSR) were recorded: instantaneous sample and moving averaged signal. A raw signal, inter-beat interval (IBI), and pulse rate were all recorded from the photoplethysmogram(PPG) sensor (pulse sensor). All signals were properly labeled. 'AF3', 'F7', 'F3', 'FC5', 'T7', 'P7', 'O1', 'O2', 'P8', 'T8', 'FC6', 'F4', 'F8', 'AF4'. Figure 1 shows the EEG representation of raw signal.

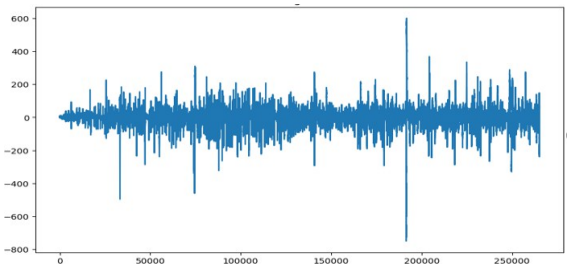

Figure 1: EEG representation of raw signal.

We used a unique pre-processing method that segmented the signals, accounting for the varying signal lengths across the dataset's tasks. This study

R., V. and Jagtap, S. S.
Analysis of Auditory Attention Based EEG Signals across Time, Frequency and Time-Frequency Domains.
DOI: 10.5220/0013938700004919

In *Proceedings of the 1st International Conference on Research and Development in Information, Communication, and Computing Technologies (ICRDICCT'25 2025) - Volume 5*, pages 606-616
ISBN: 978-989-758-777-1

examines EEG signals under various noise levels and semantic conditions, employing time, frequency, and time-frequency analyses. For this classification, we used ensemble classifiers such as AdaBoost (ADA) (Hoseini, S.S 20204). XGBoost (XGB) (Wang, F., et al., 2022) and Random Forest (RF) (Edla, D.R., et al., 2018). XGB performs better than the other two classifiers, particularly in frequency domain analysis.

2 RELATED WORKS

This section discusses a variety of Auditory attention detection task-related works. A novel neural-inspired architecture for EEG-based auditory attention detection (AAD) beat both linear and CNN models on the KUL and DTU databases, with average accuracies of 91.2% and 61.5% within 5-second windows, respectively. It demonstrated continuous improvements throughout 1 to 5-second decision windows while being much more computationally efficient (less than 1% of SSF-CNN's cost), making it appropriate for neuro-steered hearing aids. However, its accuracy lags behind the cutting-edge SSF-CNN model (Cai, S., et al., 2022) STAnet, a model for auditory spatial attention detection (ASAD), uses spatial and temporal EEG data to achieve excellent accuracy on the KUL and DTU databases (92.6% and 76.1% within 5-second windows, respectively). It works well with as few as 16 EEG channels and incorporates spatial-temporal aspects for greater accuracy. However, it may encounter overfitting or computational complexity issues (Su, E., et al., 2022) EEG-Graph Net, an EEG-graph convolutional network with a neural attention mechanism, decodes auditory attention by modeling EEG channels as nodes and their interactions as edges, so representing the brain's spatial patterns as a graph. It obtained outstanding 1-second window accuracies of 96.1% and 78.7% on the KUL and DTU databases, respectively (Cai, S., T. Schultz, and H. Li 2023). A neuronal attention mechanism has been proposed to dynamically assign weights to EEG sub-bands and channels, collecting discriminative representations for auditory attention detection (AAD). When combined with an AAD system, it achieved 1-second and 2- second average accuracies of 79.3% and 82.96% on the KUL and DTU databases, respectively. While effective, its precision falls short of previous works (Cai, S., et al., 2021). A unique Auditory Attention Decoding (AAD) mechanism was presented, which combines CNN and ConvLSTM to extract spectro-spatial-temporal information from 3D descriptors using topographical activity maps of multi-frequency bands. Experiments on KUL, DTU, and PKU databases with 0.1s, 1s, 2s, and 5s decision windows outperformed SSF-CNN and cutting-edge models. Even without auditory stimuli, the model improved AAD accuracy, with different trends observed across databases and decision windows. Multi-band frequency analysis and ConvLSTM-based temporal analysis made major contributions to the accuracy gains (Jiang et al., 2022).

As previously stated, the majority of prior classification work has used the KUL and DTU datasets; however, no work has used the PhyAAt dataset for this form of categorization. Nonetheless, some research has focused on attention score (Bajaj et al., 2022) detection tasks on the PhyAAt dataset, as described below. Study (Ahuja, C. and D. Setia 2022) enhances selective auditory attention research by combining 14-channel EEG data from the PhyAAt dataset with speech-to-text annotations. Using EEGNet and traditional machine learning, it reduced test MAE from 29.65 to 22.47 for a single individual, resulting in an overall MAE of 31.47. Incorporating speech-to-text data improves attention monitoring, but the model is prone to overfitting and lacks evaluation at various noise and semantic levels. Study (Kim, D.-Y., et al 2022) used Multivariate Multiscale Entropy (MMSE) to examine entropy variations in EEG data in relation to auditory input and attention levels. The MMSE, a measure of information in random signals, demonstrated that entropy rises during sentence practice, non-semantic sentence presentation, and when noise is combined with input sentences. These findings present a quantitative technique to assessing cognitive models. However, the emphasis on specific conditions (rehearsal, non-semantic words, noise) limits its applicability to other situations, and depending entirely on MMSE and entropy-based analysis may neglect other relevant EEG signal variables.

3 PROPOSED METHODOLOGY

To evaluate and detect task classification in the PhyAAt dataset, we used a variety of domain analyses along with ensemble classifier's. Our proposed mechanism involves three stages of work: preprocessing, feature extraction, and classification. Figure 2. represent the general block diagram of proposed work.

3.1 Unique Data segmentation Preprocessing

In this study, we used EEG signals from 25 different subjects to evaluate performance on a per-subject basis. The pre-processing, feature extraction, and classification steps were carried out consistently across all subjects. At this point, we combined signals from different noise and semantic levels for classification. Each subject's dataset includes signals from three stages: writing, listening, and resting. These signals vary in length and order, making it difficult to use traditional label-based task separation methods. This problem is further complicated by the fact that each subject's dataset contains 300,000 records, necessitating a more specialized approach to effectively handle task-wise signal separation. To minimize the complexity, we used a unique data segmentation mechanism for signal separation. This method was created specifically to handle the varying lengths and orders of EEG signals from each task (writing, listening, and resting). The analysis process includes several key steps:

1. Initial Preprocessing: We begin by carrying out fundamental data cleaning, which includes eliminating duplicates and handling missing values.
2. Label Segmentation: Unique labels are identified, and a mask is created to detect invalid entries (e.g., label: -1 = unwanted data, 0 = listening, 1 = writing, 2 = resting), which are then filtered for further analysis. Label -1 was removed, and the remaining labels (0, 1, and 2) were considered for the next process.
3. Task Segmentation: Each record is assigned a serial number, which helps in accurate separation by distinguishing various activities (writing, listening, and resting) and determining discontinuities.

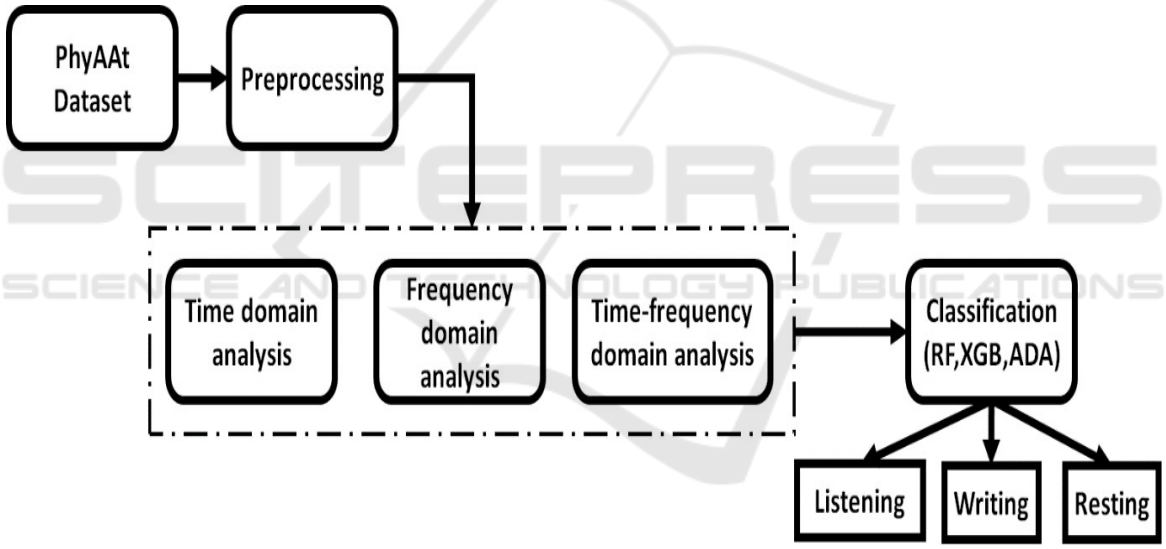

Figure 2: General block diagram of different domain auditory attention analysis.

It begins with doing the standard Exploratory Data Analysis (EDA) procedure, that involved tasks like null value detection and duplicate removal. Next, we find every unique label in the dataset. To find the entries where the label equals (-1 = unwanted data, 0 = listening, 1 = writing, and 2 = resting), which usua ly denotes invalid or noisy data, we next build a mask. Lastly, we use this mask to filter the dataset and extract the rows that have the labels (-1, 0, 1, and 2), storing them in a different variable for handling the data with the labels (0, 1, and 2) and eliminating the data with the label (-1). Before separating the task records, we added a serial number to the data in order to identify the discontinuities for each label. This serial number is used to track the continuity of the records and identify where task changes occur. By giving each record a unique identity, we may more reliably differentiate the signals associated with different jobs (writing, listening, and resting) based on the discovered discontinuities. This stage guarantees that the signals are properly segregated and isolates each task for further analysis. Once all the discontinuities are identified and the tasks are segmented, each segment undergoes feature extraction in different domains. Specifically, we extract features from the

time domain, frequency domain, and time- frequency domain.

3.2 Feature Extraction

1. Time Domain feature extraction:

In the time-domain feature extraction technique, we used raw EEG signals as input and extracted multiple statistical features such as mean, variance, standard deviation, root mean square (RMS), skewness, and kurtosis (Alazzawı, A., et al., 2024) Table 1 represents the details of statical features extraction.

Table 1: Statistical Feature Extraction.

Statistical features	Formula
Mean	$Mean = \frac{1}{N}\sum_{n=1}^{N} S_n$
Variance	$Variance = \frac{1}{N}\sum_{n=1}^{N}(S_n - Mean)^2$
Standard deviation	$std = \sqrt{\frac{1}{N}\sum_{n=1}^{N}(S_n - Mean)^2}$
Root mean Square	$rms = \sqrt{\frac{1}{N}\sum_{n=1}^{N} S_n^2}$
Skewness	$Skewness = \frac{\frac{1}{N}\sum_{n=1}^{N}(S_n - Mean)^4}{(\sqrt{\frac{1}{N}\sum_{n=1}^{N}(S_n - Mean)^2})^2}$
Kurtosis	$Kurtosis = \frac{\frac{1}{N}\sum_{n=1}^{N}(S_n - Mean)^3}{(\sqrt{\frac{1}{N}\sum_{n=1}^{N}(S_n - Mean)^2})^3}$

Where S_n represents each data point, and N is the total number of samples.

2. Frequency Domain feature extraction:

Frequency-domain evaluation involves converting time-domain EEG signals to the frequency domain via Power Spectral Density (PSD) estimation. The PSD assists identify the distribution of signal power among different frequency components. After obtaining the PSD, we extract statistical features including mean, variance, standard deviation, RMS, skewness, and kurtosis, which were used in the time-domain analysis. Integrating alpha, beta, and gamma band power analysis with these statistical features gives us a deeper comprehension of the EEG signal. The

combined method gathers both statistical

3. Time-Frequency domain feature extraction:

Discrete Wavelet Transform (DWT): We apply the Discrete Wavelet Transform (DWT) with 'db2' (Daubechies wavelet with 2 vanishing moments) as the selected wavelet in order to analyze the EEG signals in the time-frequency domain. A mathematical method called the Discrete Wavelet Transform (DWT) is used to convert a signal into a wavelet-based representation. It is especially helpful for analyzing non-stationary signals like EEG, where both frequency content and time localization are crucial, because it offers both time and frequency information (Pattnaik et al., 2016).

4 RESULTS AND DISCUSSION

In this section, we perform the experiments ten times in order to increase the robustness and reliability of the classifier. The three ensemble classifiers performance (Ada, XGB, and RF) was examine d using the mean accuracy and standard deviation. Table 2 shows the performance of the classifiers on time, frequency, and time-frequency domain evaluation for all 25 subjects.

4.1 Time Domain

The time domain evaluation showed that the XGB and RF performed better than the ADA boost classifier. For subjects 2, 6, 7, 9, 10, 11, 12, 15, 16, 17, 18, and 25, RF outperformed XGB and ADA boost classifiers. However, XGB only provided approximate RF performance for those subjects. On the other hand, subjects 1,3,4,5,8,13,14,19,20,21,22, 23, and 24 XGB outperformed RF and ADA boost classifiers. The accuracy of XGB beat RF and ADA, indicating that the model is better at recognizing EEG signals. Subject 5 obtained the highest accuracy of 89.77%, while subject 10 had a minimum accuracy of 64.34%.

Table 2: Performance analysis of the classifiers on time, frequency and time- frequency domain analysis for all 25 subjects.

Sub /Metrics		Time domain			Frequency domain			Time-frequency domain		
		RF	XGB	ADA	RF	XGB	ADA	RF	XGB	ADA
S1	Mean Accuracy	82.97	83.75	75	84.22	85.55	81.48	79.92	76.88	70.08
	Std deviation	0.025	0.028	0.036	0.031	0.031	0.031	0.024	0.035	0.038
S2	Mean Accuracy	81.48	81.48	73.05	84.22	85.55	81.48	79.14	78.44	66.64
	Std deviation	0.017	0.027	0.041	0.031	0.031	0.031	0.027	0.047	0.026
S3	Mean Accuracy	75.58	76.43	68.7	80.16	81.01	73.18	76.82	74.26	66.36
	Std deviation	0.034	0.035	0.053	0.023	0.024	0.033	0.025	0.031	0.032
S4	Mean Accuracy	65.43	66.59	61.78	62.17	59.61	57.05	62.79	62.4	61.01
	Std deviation	0.031	0.035	0.02	0.033	0.037	0.025	0.047	0.029	0.042
S5	Mean Accuracy	86.56	89.77	86.95	84.3	87.27	75.7	86.88	89.06	85.39

	Std deviation	0.024	0.028	0.026	0.028	0.026	0.06	0.029	0.025	0.051
S6	Mean Accuracy	88.14	87.75	83.72	91.94	90.39	83.57	86.9	88.53	84.88
	Std deviation	0.018	0.014	0.043	0.015	0.023	0.04	0.019	0.02	0.02
S7	Mean Accuracy	72.79	71.63	63.88	76.59	78.22	71.01	76.9	75.81	69.3
	Std deviation	0.37	0.032	0.035	0.03	0.03	0.03	0.033	0.035	0.048
S8	Mean Accuracy	71.16	71.55	63.95	80.23	78.6	71.55	73.64	71.86	62.02
	Std deviation	0.031	0.032	0.337	0.023	0.309	0.041	0.04	0.033	0.041
S9	Mean Accuracy	80.08	79.22	72.25	86.2	85.43	83.72	81.4	80.39	75.89
	Std deviation	0.034	0.033	0.035	0.024	0.027	0.042	0.033	0.023	0.035
S10	Mean Accuracy	64.34	62.48	61.55	71.55	72.33	62.56	68.14	67.6	57.91
	Std deviation	0.032	0.032	0.035	0.033	0.031	0.051	0.028	0.03	0.041
S11	Mean Accuracy	82.95	81.4	77.21	79.53	80.00	72.64	72.71	70.54	65.27
	Std deviation	0.024	0.028	0.036	0.019	0.031	0.039	0.047	0.031	0.024
S12	Mean Accuracy	65.81	64.11	57.67	74.16	72.25	67.67	71.16	65.97	62.25
	Std deviation	0.034	0.04	0.053	0.013	0.027	0.038	0.025	0.042	0.042
S13	Mean Accuracy	73.49	74.37	69.15	79.69	78.29	70.54	77.29	75.89	73.8
	Std deviation	0.029	0.031	0.035	0.028	0.035	0.037	0.023	0.013	0.052
S14	Mean Accuracy	81.71	84.34	74.73	82.33	80.08	73.18	78.14	78.45	73.57
	Std deviation	0.03	0.025	0.07	0.033	0.032	0.063	0.031	0.032	0.027
S15	Mean Accuracy	69.69	69.15	64.73	85.53	84.65	79.3	67.75	64.57	58.37
	Std deviation	0.02	0.049	0.071	0.033	0.021	0.025	0.036	0.045	0.034

S16	Mean Accuracy	65.89	64.11	61.94	64.19	65.5	59.84	69.22	67.29	62.48
	Std deviation	0.029	0.029	0.048	0.027	0.013	0.039	0.024	0.024	0.031
S17	Mean Accuracy	74.73	74.19	70.47	79.61	78.84	74.96	73.72	69.92	65.81
	Std deviation	0.031	0.032	0.043	0.023	0.027	0.023	0.023	0.027	0.028
S18	Mean Accuracy	88.53	87.75	78.14	85.35	84.34	76.51	84.57	82.56	73.88
	Std deviation	0.007	0.027	0.034	0.016	0.023	0.031	0.024	0.024	0.065
S19	Mean Accuracy	71.01	73.1	69.3	72.79	70.00	65.89	70.78	69.84	67.98
	Std deviation	0.038	0.024	0.035	0.037	0.025	0.046	0.031	0.044	0.042
S20	Mean Accuracy	87.05	87.67	77.44	88.37	86.43	84.11	83.64	81.71	73.18
	Std deviation	0.025	0.022	0.072	0.027	0.032	0.041	0.024	0.029	0.045
S21	Mean Accuracy	74.5	77.98	64.34	79.84	81.63	73.57	74.73	73.02	64.26
	Std deviation	0.029	0.034	0.031	0.029	0.038	0.044	0.021	0.039	0.031
S22	Mean Accuracy	68.14	68.91	61.24	78.37	79.22	73.26	72.02	68.06	65.12
	Std deviation	0.034	0.028	0.05	0.019	0.04	0.032	0.016	0.051	0.035
S23	Mean Accuracy	67.75	67.91	57.6	75.5	75.04	69.15	68.06	64.73	60.08
	Std deviation	0.027	0.09	0.027	0.036	0.035	0.057	0.045	0.023	0.031
S24	Mean Accuracy	56.12	58.29	52.4	60.78	57.75	54.88	61.24	57.8	51.4
	Std deviation	0.042	0.034	0.041	0.045	0.025	0.03	0.043	0.026	0.033
S25	Mean Accuracy	83.64	82.33	77.36	84.88	85.19	81.09	79.69	78.76	74.81
	Std deviation	0.025	0.028	0.041	0.029	0.012	0.031	0.034	0.027	0.032
	Average Accuracy	75.1816	75.4504	68.982	78.9	78.5268	72.7156	75.09	73.3736	67.6696

Figure 3 and 4 represent the confusion matrices and ROC curves for RF, XGB, and Ada classifiers, respectively. From these confusion matrix results, it is evident that RF effectively classifies the listening task, XGB shows superior performance in classifying the resting task, and AdaBoost excels in classifying the writing task compared to the other two tasks. Among the three tasks, the ROC curves indicate that the writing task consistently shows superior performance across all classifiers when compared to resting and listening task.

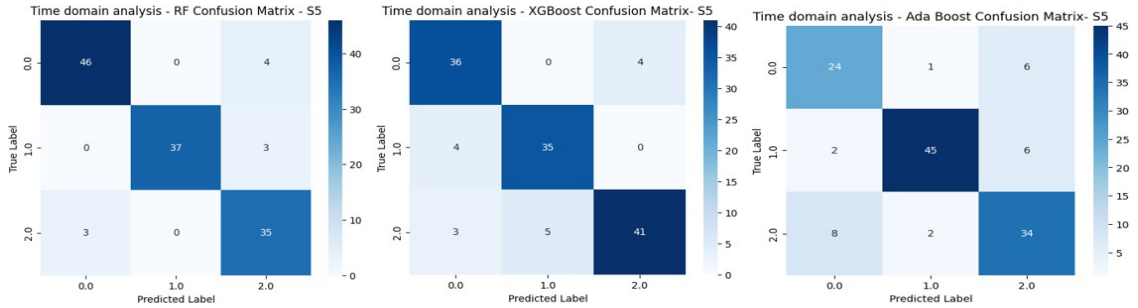

Figure 3: Confusion matrix for RF, XGB and ADA. (Time domain).

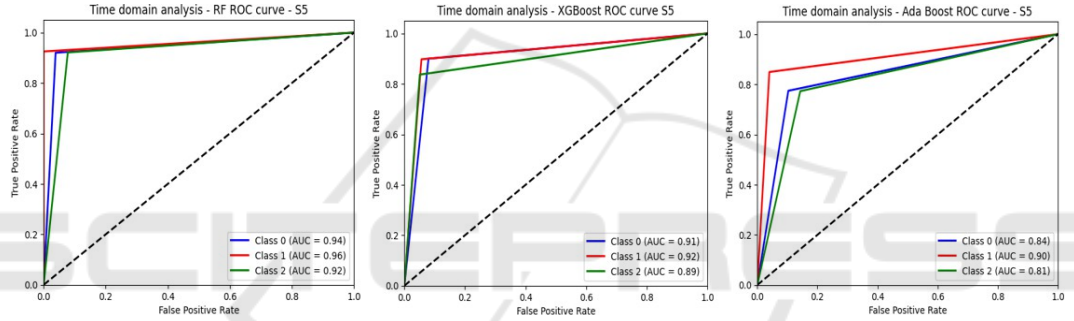

Figure 4: ROC curve for RF, XGB and ADA. (Time domain).

4.2 Frequency Domain

In the time domain evaluation XGB and RF performed better than the ADA boost classifier. In subjects 4, 6, 8, 9, 12, 13, 14, 15, 17, 18, 19, 20, 23, 24, and 25, RF outperformed XGB and ADA boost classifiers. However, in subjects 1, 2, 3, 5, 7, 10, 11, 16, 21, and 22, XGB outperformed RF and ADA boost classifiers. RF beat both XGB and ADA suggesting that the model is more efficient at recognizing EEG signals in the frequency domain. Subject 6 achieved the highest accuracy in frequency domain analysis (91.99%), while subject 24 had the lowest accuracy (60.78%). Figure 5 and 6 present the confusion matrices and ROC curves for RF, XGB, and Ada classifiers, respectively on frequency domain. From the confusion matrix results, it is evident that all classifiers perform equally well in classifying the listening, writing, and resting tasks in the frequency domain analysis. Among the three tasks, the ROC curves indicate that the listening task consistently shows superior performance across all classifiers when compared to resting and wring task in frequency domain analysis.

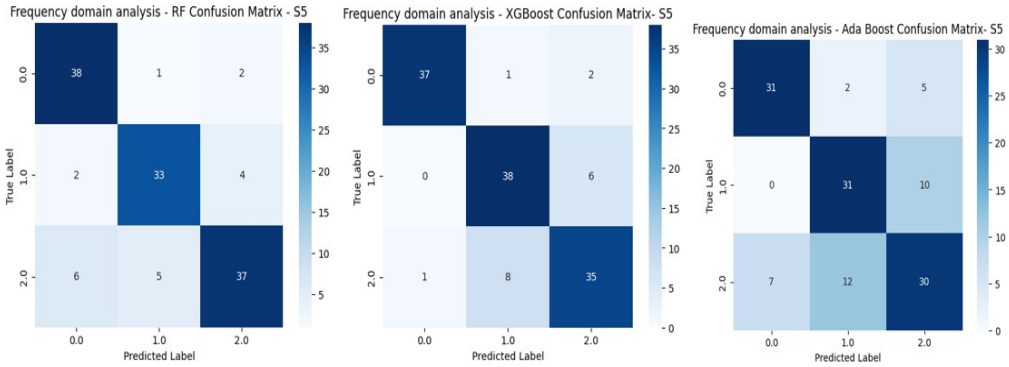

Figure 5: Confusion matrix for RF, XGB and ADA. (Frequency domain).

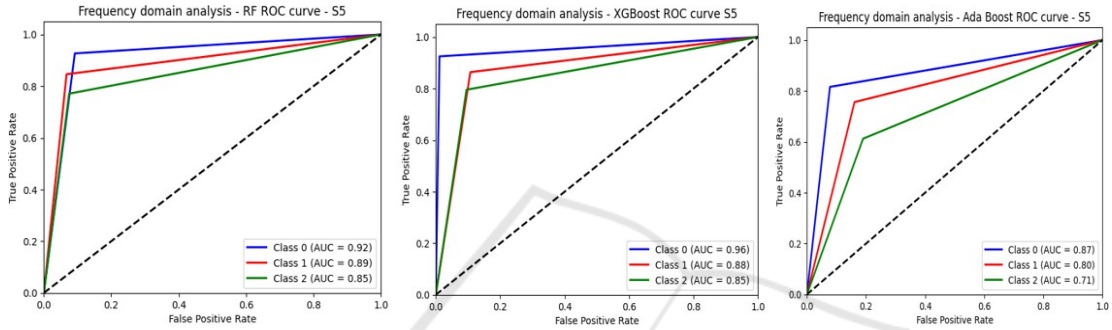

Figure 6: ROC curve for RF, XGB and ADA. (Frequency domain).

4.3 Time-Frequency Domain

In the time-frequency domain, the RF and XGB performed better than the ADA boost classifier. In subjects 1, 2, 3, 4, 7, 8, 9, 10, 11, 12, 13, 15, 16, 17, 18, 19, 20, 21, 22, 23, 24, and 25, RF outperformed XGB and ADA boost classifiers. For those subjects, XGB only produced an approximate RF performance. However, XGB outperformed RF and ADA boost classifiers in subjects 5, 6, and 14. Both XGB and AdaBoost were surpassed in accuracy by RF, indicating that the model is more successful in accurately classifying the EEG signals in the time - frequency domain. Subject 5 achieved the highest accuracy of 89.05% in frequency domain analysis, while subject 24 had the lowest accuracy of 61.24%. Figure 7 and 8 present the confusion matrices and ROC curves for RF, XGB, and Ada classifiers, respectively on time-frequency domain. From these confusion matrix results, it is evident that RF effectively classifies the resting task, XGB shows superior performance in classifying the listening task, and AdaBoost excels in classifying the writing task compared to the other two tasks. Among the three tasks, the ROC curves indicate that performed equally well in classifying the listening, writing, and resting tasks in the time-frequency domain analysis.

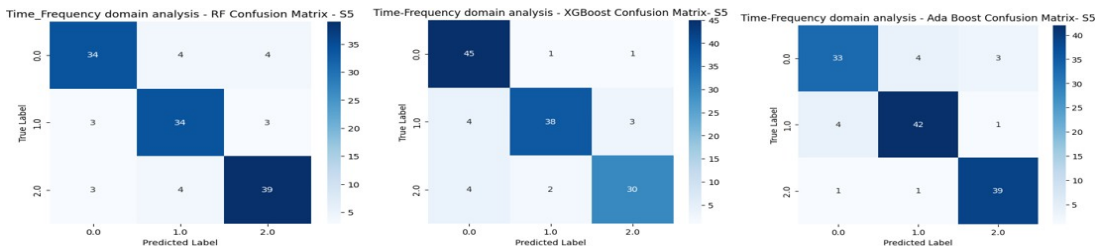

Figure 7: Confusion matrix for RF, XGB and ADA (Time-Frequency domain).

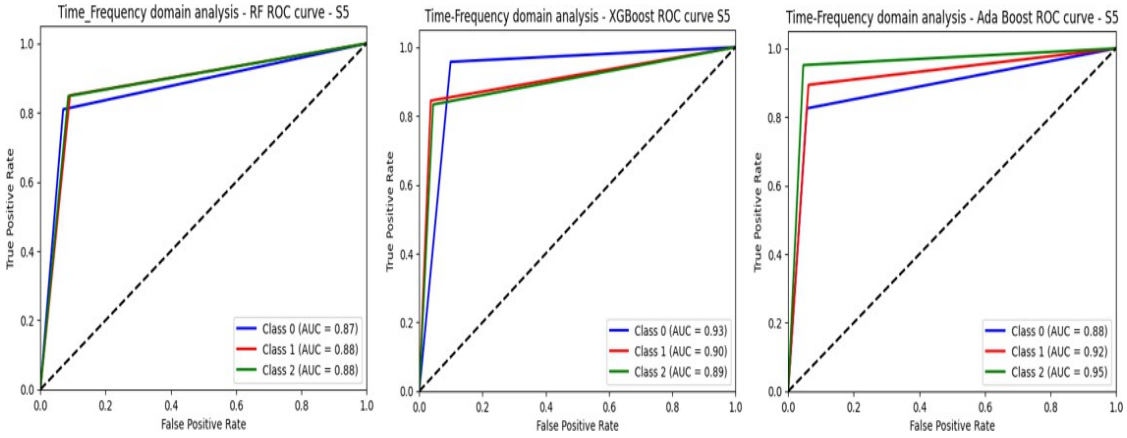

Figure 8: ROC curve for RF, XGB and ADA. (Time-Frequency domain).

In the time, frequency, and time-frequency domains, XGB and RF performed better than AdaBoost on average, according to the three classifiers' analysis. However, XGB performed better in terms of false positives and false negatives. Our analysis showed that Subject 5 outperformed the other subjects. This superior performance was maintained in all three domains. Subject 24 had the lowest classification performance among all the subjects. For this subject, the time-frequency domain was the only analysis method that showed a significant improvement in performance. Unlike the time and frequency domains, which struggled to distinguish between tasks, the time-frequency domain was able to capture key signal characteristics, resulting in improved classification accuracy. This indicates that for subjects with lower performance in time and frequency evaluations, the time-frequency analysis offers a more robust technique for gathering and identifying EEG signal patterns.

5 CONCLUSIONS

The research found that using time, frequency, and time-frequency domain evaluations on EEG data showed major variations in effectiveness of task classification (listening, writing, and resting) across all subjects. According to the results, subject 5 achieved the highest scores of 89.77%, 87.27%, and 89.06%, on time, frequency and time-frequency domains respectively. Reliable task classification required only features taken from the frequency and time domains. Alternatively, Subject 24 carried out lowest performance, with significant gains mostly in the time-frequency domain. This finding highlights the importance of time-frequency analysis in detecting complex signal features, particularly when time or frequency domain feature s are insufficient. In summary, incorporating time-frequency domain analysis demonstrated to be a powerful approach for improving classification accuracy across diverse subjects by tackling the variability in individual EEG signal patterns. Future research will focus on classifying tasks based on different noise and semantic levels to better understand the ways they affect EEG signal patterns. Additionally, by finding and employing the most relevant EEG channels, we seek to use channel selection strategies to improve classification performance.

REFERENCES

A. Alazzawi et al., “Schizophrenia diagnosis based on diverse epoch size resting-state EEG using machine learning,” PeerJ Comput. Sci., vol. 10, p. e2170, 2024.

B. Scharf, Auditory Attention: The Psychoacoustical Approach, in Attention, Psychology Press, 2016, pp. 75–117.

C. Ahuja and D. Setia, “Measuring human auditory attention with EEG,” in Proc. 14th Int. Conf. on Communication Systems & Networks (COMSNETS), IEEE, 2022. DOI: 10.1109/COMSNETS53615.2022.9668363.

D. R. Edla et al., “Classification of EEG data for human mental state analysis using Random Forest classifier,” Procedia Comput. Sci., vol. 132, pp. 1523–1532, 2018. DOI: 10.1016/j.procs.2018.05.116.

D.-Y. Kim et al., “Cognitive modeling using multivariate multiscale entropy analysis of EEG: Entropy changes according to auditory inputs and the level of attention,” in Proc. IEEE Int. Conf. on Consumer Electronics-Asia (ICCE-Asia), IEEE, 2022. DOI: 10.1109/ICCE-Asia57006.2022.9954710.

E. Su et al., "STAnet: A spatiotemporal attention network for decoding auditory spatial attention from EEG," IEEE Trans. Biomed. Eng., vol. 69, no. 7, pp. 2233–2242, 2022. DOI: 10.1109/TBME.2022.3140246.

F. Wang et al., "An ensemble of XGBoost models for detecting disorders of consciousness in brain injuries through EEG connectivity," Expert Syst. Appl., vol. 198, p. 116778, 2022. DOI: 10.1016/j.eswa.2022.116778.

M. Val-Calvo et al., "Real-time multi-modal estimation of dynamically evoked emotions using EEG, heart rate and galvanic skin response," Int. J. Neural Syst., vol. 30, no. 4, p. 2050013, 2020. DOI: 10.1142/S0129065720500136.

N. Bajaj, J. R. Carrión, and F. Bellotti, "Phyaat: Physiology of auditory attention to speech dataset," arXiv preprint arXiv:2005.11577, 2020.

N. Bajaj, J. R. Carrión, and F. Bellotti, "Deep representation of EEG data from spatio-spectral feature images," arXiv preprint arXiv:2206.09807, 2022.

S. Pattnaik, M. Dash, and S. Sabut, "DWT-based feature extraction and classification for motor imaginary EEG signals," in Proc. Int. Conf. on Systems in Medicine and Biology (ICSMB), IEEE, 2016.

S. Cai et al., "EEG-based auditory attention detection via frequency and channel neural attention," IEEE Trans. Hum.-Mach. Syst., vol. 52, no. 2, pp. 256–266, 2021. DOI: 10.1109/THMS.2021.3125283.

S. Cai et al., "A neural-inspired architecture for EEG-based auditory attention detection," IEEE Trans. Hum.-Mach. Syst., vol. 52, no. 4, pp. 668–676, 2022. DOI: 10.1109/THMS.2022.3176212.

S. Cai, T. Schultz, and H. Li, "Brain topology modeling with EEG-graphs for auditory spatial attention detection," IEEE Trans. Biomed. Eng., 2023. DOI: 10.1109/TBME.2023.3294242.

S. S. Hoseini, "Enhancing anxiety diagnosis through ADA BOOST-assisted decision-level fusion," J. Curr. Trends Comput. Sci. Res., vol. 3, no. 3, pp. 1–10, 2024.

W. B. Ng et al., "PSD-based features extraction for EEG signal during typing task," IOP Conf. Ser.: Mater. Sci. Eng., vol. 557, no. 1, p. 012032, 2019. DOI: 10.1088/1757-899X/557/1/012032.

Y. Jiang, N. Chen, and J. Jin, "Detecting the locus of auditory attention based on the spectro-spatial-temporal analysis of EEG," J. Neural Eng., vol. 19, no. 5, p. 056035, 2022. DOI: 10.1088/1741-2552/ac975c.